Study on the origins of residual stresses in Ti-6Al-4V processed by additive manufacturing

Nathan Dumontet[1,*], Benoit Malard[1] and Bernard Viguier[1]

[1] CIRIMAT, Université de Toulouse, CNRS, INP- ENSIACET 4 allée Emile Monso - BP44362, 31030 Toulouse Cedex 4 – France

[*]nathan.dumontet@ensiacet.fr

Abstract

In additive manufacturing processes using laser beam melting high thermal gradients are generated, inducing residual stresses within the parts that may lead to deformations and, in worst cases, cracks. One of the materials that is the most sensitive to residual stresses is the Ti-6Al-4V alloy. In the present study, we focus on the various parameters that may control the genesis and build-up of the residual stress states. Dwell time and thermal conductivity, both influencing the heat evacuation, were studied. Higher thermal evacuation was find to rises residual stresses within the part. Then, the reliability of the energy density as a comparison parameter was investigated. Samples with the same energy densities but different power and scanning speed were elaborated. Energy density was shown as a non-reliable parameter to compare different processed parts.

Introduction

Residual stresses (RS) encountered in additive manufacturing, and more precisely in laser beam melting (LBM), are still a problem in the conception of titanium parts and their origins are not well understood. Because of the laser high energy a high thermal gradient is induced in the material, reaching 10^7 $K.m^{-1}$ [1] leading to large RS [2,3]. A lot of work is done to simulate the LBM process in order to understand the thermal gradient that lead to RS [4,5].This study aims at experimentally investigate the effect of different parameters on the thermal gradient in order to understand the origins of RS in the Ti-6Al-4V (Ti64). The energy density is a value widely used in the literature, but dependent of numerous parameters such as the laser power or the scanning speed. In order to study the reliability of the energy density as a comparison parameter, samples with the same energy density but with different scanning speed and power were processed. Energy density is defined as:

$$E = \frac{P}{vht}$$

with P the laser power; v the scanning speed; h the laser diameter and t the powder bed thickness [6]. Parameters involving the heat evacuation like the dwell time (which is the time between the processing of two successive layers of the same part) or the thermal conductivity were studied. Dwell time is showed to be involved in RS building even if it is not really clear in the case of the Ti64 [7].

Manufacturing and characterizations

Samples were processed in bridges shapes [8] in order to generate a large RS state using a Phenix ProX200 with a recycled powder of Ti64. Those bridge samples are 8 mm high, 10 mm wide and 20 mm long. Different parameters were used in order to study the origins of RS. Constructor parameters for Ti64 powders are: power 300 W, scanning speed 1800 mm/s, layer thickness of 60 µm and laser diameter of 70 µm with a zig-zag scanning pattern and a 90° hatch angle (which is the angle between the patterns of two successive layers). Five energy densities where chosen using the literature [9] and default parameters, then three couples of power and scanning speed were selected for each energy density. Problems were encountered during the processing of some samples and results shown here are only from two energy densities: 47.62 J/mm^3 and 31.75 J/mm^3. All the conditions tentatively used to elaborate samples are plotted in Figure 1, corresponding to four density energies values (lines). In this plot filled symbols represent successful manufacturing and open symbols indicate unsuccessful fabrication.

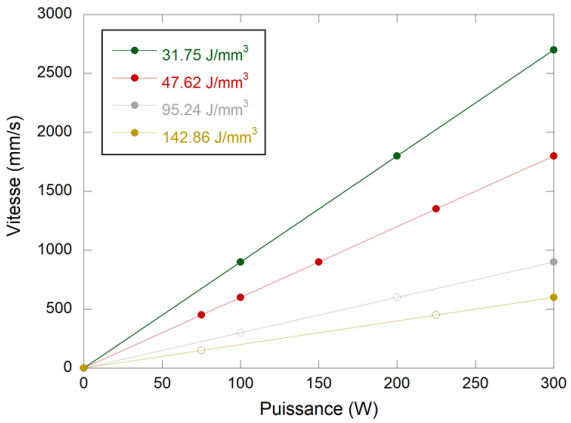

Figure 1 – Energy densities studied. Samples that failed are marked by open symbols and samples processed by filled symbols.

Four different batches were processed in order to study RS origins. The first and second batches differ only by the difference in the materials chosen for the baseplate. Titanium for the first and aluminum for the second. On these batches are manufactured two bridges at the same position and with the same default parameters. On third and fourth batches, both baseplates in titanium, nine samples were built as well as the two references bridges at the same position than the first and second batches. Those nine samples were divided in three energy densities and each sample possesses a different couple of power and scanning speed. So three couples by energy density.

In order to determine the RS state on top of samples, laboratory X-Ray Diffraction (XRD) is used. In order to study them under laboratory X-Ray a dense support was built under the bridge to maintain the RS state even after separation of the sample with the baseplate (figure 2a).

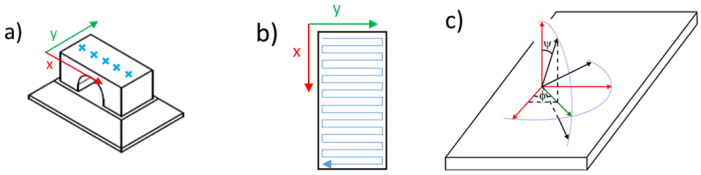

Figure 2 – a) Location of the points measured on the samples; b) Pattern formed by the laser on the last layer built; c) Angles φ and ψ marking the directions along which strain is measured by XRD

XRD was performed using a Bruker D8-Discover with a cobalt micro-source (λ= 1.793 A), a spot size of 1 mm and a 2D detector. With a cobalt sources the penetration length in the Ti64 is about 3 µm. To access the RS tensor the $\sin^2\psi$ method was used [10], involving the measurement of the strain along different directions marked by angles φ and ψ. Directions φ and ψ angles are represented in figure 2c. It is shown in literature that the α' phase behave differently than the α phase in terms of elasticity [11] thus X-ray elastic constants used in this study are those from the α' martensitic phase: S_1 = -3.25 10^{-6} MPa^{-1} and $^1/_2S_2$ = 11.40 10^{-6} MPa^{-1} [12].

Stress tensors where determined in five points on the top surface of bridges as represented in figure 2a, along four different ψ angles (0°, 20°, 40° and 60°) and three φ angles (0°, 45° and 90°) with an acquisition time of 20 minutes per direction, leading to 20 hours per samples. This strategy allowed us to access the RS tensor along two perpendicular directions: σ_x along the long axis (x) of the bridge and σ_y along the short axis (y). As the last processed layers has a weld bead along the short axis (y), as represented in figure 2b, it is expected to have stronger residual stresses along σ_y [13]. Density measurements where performed with the Archimedes method using a KERN ARJ 220-4m.

Results and discussions

Are given in table 1 the RS determined by XRD for each reference sample from every batch, baseplate material and dwell time. XRD results given here are the average of the five points measured on top of samples. Δt is the dwell time of the last layer, calculated with time needed to build the last layers of each samples in a given batch. Reference samples are found in every batch at the same position and built with the exact same parameters.

Table 1 – Residual stresses measured by X-Ray diffraction, baseplates material and dwell time for each sample from the different batches

Batch	Baseplate	Δt (s)	Sample	σ_x (MPa)	σ_y (MPa)
1	Ti	7.61	1	86 +/- 27	309 +/- 28
			2	97 +/- 26	271 +/- 27
2	Al	7.61	1	117 +/- 35	300 +/- 36
			2	186 +/- 28	335 +/- 29
3	Ti	22.43	1	176 +/- 25	358 +/- 25
			2	183 +/- 25	390 +/- 26
4	Ti	20.25	1	150 +/- 28	298 +/- 28
			2	189 +/- 31	372 +/- 32

The first stricking result is that σ_y values are systematically higher than σ_x. This is related to the last layer being built with the longer scanning direction along y and the thermal gradient being larger along the weld bead [13]. RS of the samples from the first batch are described (two references on a titanium plate). RS were measured at 92+/-27 MPa for σ_x and 290+/-27 MPa for σ_y on average for the 2 references on the five points of bridges. In comparison, the average stresses samples on the aluminum baseplate reached 151+/-32 MPa for σ_x and 320+/33 MPa for σ_y. Those samples were in the same position with the same powder and built with the same parameters than those of the first batch. The only difference between those samples was the material of the baseplate. First one was titanium while second was aluminum. Pure titanium has a thermal conductivity around 20 W/(m.K) while it is around 237 W/(m.K) for pure aluminum. Therefore, meanwhile heat evacuation was enhanced by the aluminum baseplate, RS raised. Indeed, heat evacuation rises the difference in temperature between the top and the bottom of the sample, increasing the thermal gradient in the sample. From high thermal gradient, inhomogeneous thermal dilatation appears, leading to higher RS. This result can be compared to a heated baseplate. Indeed, while heating a base plate, the thermal gradient is reduced leading to lower RS [14]. In opposition, raising the thermal conductivity cools down the baseplate and increases RS. On the third batch, σ_x was 180+/-25 MPa and σ_y around 374+/-24 MPa in average for the reference samples. For the fourth batch, it was 170+/-29 MPa for σ_x and 335+/-30 MPa. On those baseplate nine more samples were fabricated than on the first baseplate. Increasing the number of part processed means rising the dwell time. Dwell time is difficult to estimate because it changes for every layer has the processed surface evolves through the height. Rising the dwell time allows a longer heat evacuation time. This also increases the thermal gradient, leading to higher RS state. In either cases, thermal conductivity or dwell time, when the heat evacuation is made easier a larger RS state is observed on top of the finished sample. Samples processed with different couple of scanning speed and power but same energy densities showed different RS states. In figure 2 is given the example for E = 47.62 J/mm^3. The same behavior was observed for samples from other energy densities.

The average of the five points measured on the surface of each sample is used. When rising couples of scanning speed and power, RS accessed first rises then decreases. In figure 3 one can see that the lowest density is observed for the sample with couples of lower scanning speed and power. Pores in the material reduces RS because of the free surface. This is why low RS states are observed in samples with low velocity and power.

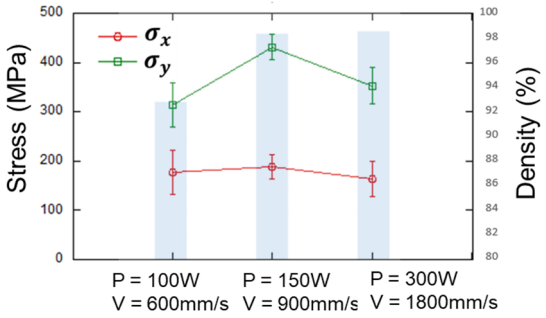

Figure 3 – Density measurements in comparison with RS determined for the three samples build with an energy density of 47.62 J/mm³

In samples with high velocity and power an effect of the scanning speed can be expected. Indeed, when the velocity is high the dwell time is reduced, leading to a lesser heat evacuation time. As seen with dwell time, increasing the scanning speed will lower the RS state. One can see here that the energy density cannot be used as a comparison parameter. Indeed, it is demonstrated that with the same energy density different couples of velocity/power lead to different RS states.

Conclusion

This study enhanced the understanding of the origins of RS in additive manufacturing of the Ti64 alloy. Different parameters such as the scanning speed, velocity and heat evacuation were investigated and some answers were given:

- As RS are mostly induced by thermal gradient in additive manufacturing, heat evacuation was found to have a strong effect on their origins. By increasing dwell time or thermal conductivity of the baseplate it was found that easier the heat is evacuated, stronger RS are.
- Energy density was kept constant on various samples by changing laser speed and power. Samples with the same energy density where found to have different RS states. This study exposed the density energy as a non-reliable comparison parameters.

Bibliography

[1] B. Vrancken, V. Cain, R. Knutsen, J. Van Humbeeck, Scripta Mater. 87 (2014) 29-32

[2] Y. Liu, Y. Yang, D. Wang, Int. J. Adv. Manuf. Technol. 87 (2016) 1-10

[3] A. Vasinonta, J. Beuth, M. Griffith, In Solid Freeform Fabrication Proceedings. (2000) 200-208

[4] T. Mukherjee, H.L. Wei, A. De, T. DebRoy, Comput. Mater. Sci. 150 (2018) 304-313

[5] T. Mukherjee, H.L. Wei, A. De, T. DebRoy, Comput. Mater. Sci. 150 (2018) 369-380

[6] L. Thijs, F. Verhaeghe, F. Craeghs, J. Van Humbeeck, J.P. Kruth, Acta. Mater. 58 (2010) 3303-3312

[7] E.R. Denlinger, P. Michaleris, Addit. Manuf. 12, *Part A*, (2014) 51-59

[8] J.P. Kruth, J. Deckers, E. Yasa, R. Wauthlé, Proc. Inst. MEch. Eng. Part B J. Eng. Manuf. 226 (2012) 980-991

[9] B. Song, S. Dong, B. Zhang, H. Liao, C. Coddet, Mater. Des. 35 (2012) 120-125

[10] H. Dolle, V. Hauk, Härt.-Tech. (1976) 165-168

[11] N. Dumontet, D. Connétable, B. Malard, B. Viguier, Scripta Mater. 167 (2019) 115-119

[12] N. Dumontet, G. Géandier, F. Galliano, B. Viguier, B. Malard, Residual Stresses 2018 – ECRS-10 (2018) 289-294

[13] L. Parry, I.A. Ashcroft, R.D. Wildman, Addit. Manuf. 12, *Part A*, (2016) 1-15

[14] N.E. Hodge, R.M. Ferencz, R.M. Vignes, Addit. Manuf. 12 (2016) 115-168